

Decoupling Substrate Stiffness, Spread Area, and Micropost Density: A Close Spatial Relationship between Traction Forces and Focal Adhesions

Sangyoon J. Han,[†] Kevin S. Bielawski,[†] Lucas H. Ting,[†] Marita L. Rodriguez,[†] and
Nathan J. Sniadecki^{†‡}

[†]Department of Mechanical Engineering and [‡]Department of Bioengineering, University of Washington,
Seattle, Washington

Figure S1

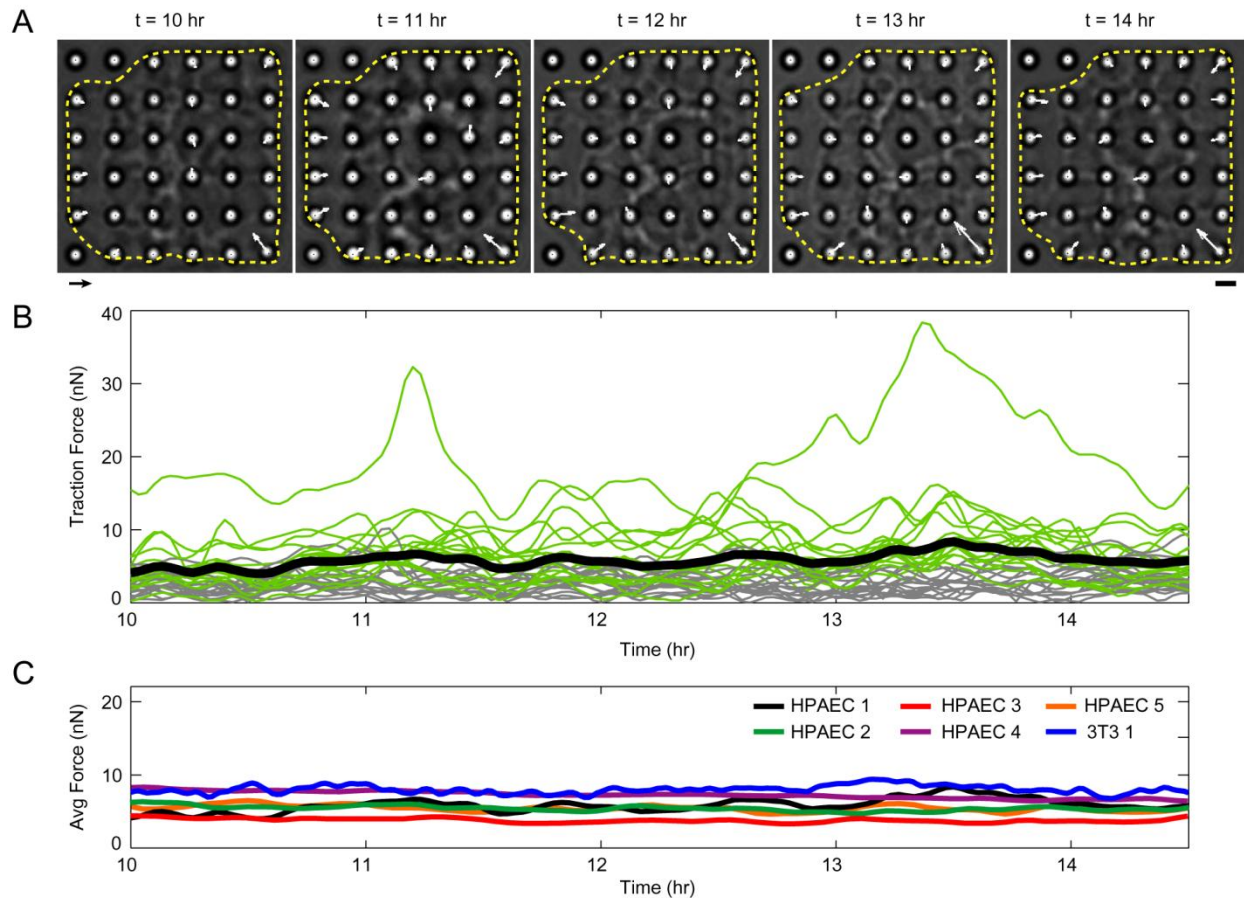


Figure S1. Traction forces of confined cells do not change significantly after 10 hr on the posts (A) Phase-contrast time-lapse images of an HPAEC, outlined in yellow dotted line, on posts with force vectors from 10 hr to 14 hr after seeding. Force scale at the lower left corner represents 10 nN while line scale at the lower right corner is $3 \mu\text{m}$. (B) Plot of the magnitudes of all traction forces under the cell in panel A as a function of time. Green lines are forces at the cell periphery while gray lines are forces at cell interior. Note that individual traction forces fluctuated over time, but the average force per post, shown as a thick black line, remained relatively constant. (C) Average forces over time for 6 cells show that average traction forces remain steady after 10 hr on the posts.

Figure S2

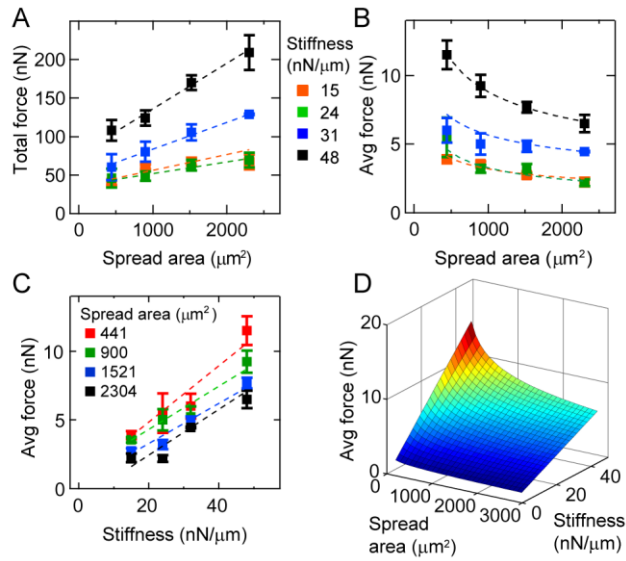


Figure S2. Spread area and post stiffness influence traction forces independently in 3T3 cells. (A) Total force increases with spread area for cells on each array type. (B) Average force decreases with spread area for each array stiffness. (C) Average force increases with substrate stiffness for each patterned area. Table S8 shows the number of cells that were measured per condition and R^2 values of the best-fit lines. (D) A multi-parameter fit of the data for average force shows they are a function of both spread area and stiffness. Table 1 shows the fit coefficient for nonlinear regression analysis.

Figure S3

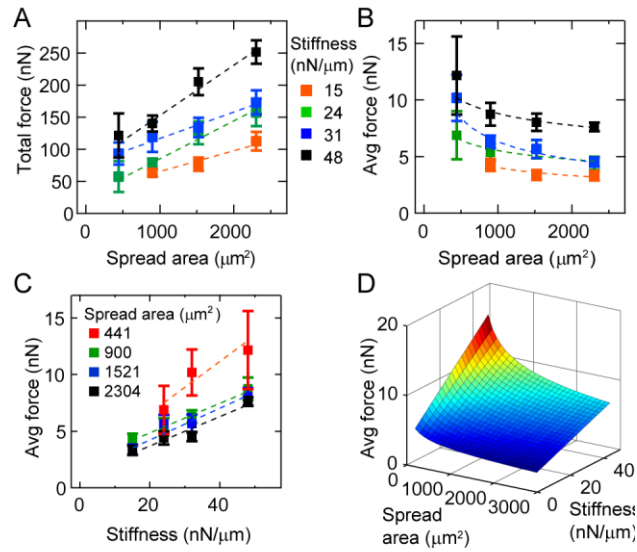


Figure S3. Spread area and post stiffness influence traction forces independently in human aortic smooth muscle cells. (A) Total force increases with spread area for cells on each array type. (B) Average force decreases with spread area for each array stiffness. (C) Average force increases with substrate stiffness for each patterned area. Table S9 shows the number of cells that were measured per condition and R^2 values of the best-fit lines. (D) A multi-parameter fit of the data for average force shows they are a function of both spread area and stiffness. Table 1 shows the fit coefficient for nonlinear regression analysis.

Figure S4

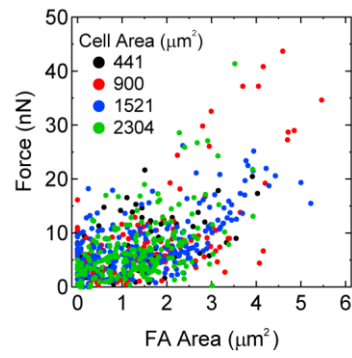


Figure S4. Individual forces at each post show a weak correlation with focal adhesion area, regardless of cell spread area. Data of force and focal adhesion area are from cells on posts with $31 \text{ nN}/\mu\text{m}$.

SI Tables

The purpose of the supplemental tables is to provide information on the dimensions of the arrays (Table S1) and the statistical data of the regression analyses (Table S2-12).

Table S1. Dimensions and stiffness of micropost arrays. Values shown in the first two rows are means \pm standard deviations. Values shown in the last two rows are means \pm error as determined by the propagation of uncertainty in the measurements for height and diameter of the microposts and elastic modulus of PDMS. From these measurements, arrays #1 through #5 were found to have spring constants that were unique from each other ($p < 0.05$, ANOVA with Tukey's post-hoc test), while arrays #4 and #6 were found to be similar to each other.

Array	#1	#2	#3	#4	#5	#6
Height, h (μm)	8.96 ± 0.36	7.44 ± 0.28	7.19 ± 0.22	7.45 ± 0.20	6.7 ± 0.13	5.62 ± 0.14
Diameter, D (μm)	2.14 ± 0.03	2.04 ± 0.06	2.22 ± 0.10	2.42 ± 0.05	2.5 ± 0.07	2.07 ± 0.05
Spacing, s (μm)	9	9	9	9	9	6
Post Stiffness, k ($\text{nN}/\mu\text{m}$)	10.7 ± 2.3	15.5 ± 3.6	24.1 ± 6.3	30.5 ± 6.2	47.8 ± 10	38.1 ± 7.9
Effective Modulus (kPa)	0.79 ± 0.15	0.95 ± 0.20	1.42 ± 0.36	1.87 ± 0.35	2.64 ± 0.55	3.96 ± 0.75

Table S2. Linear regression analysis of total force of unconfined cells versus spread areas for each type of stiffness reported in Figure 1 C.

Stiffness ($\text{nN}/\mu\text{m}$)	Number of points	Slope ($\text{nN}/\mu\text{m}^2$)	Slope Error ($\text{nN}/\mu\text{m}^2$)	Intercept (nN)	Intercept Error (nN)	R^2
11	30	0.056	0.013	27.86	15.76	0.40
15	33	0.050	0.008	35.59	10.22	0.55
24	31	0.079	0.006	86.34	10.72	0.85
31	35	0.085	0.013	76.79	24.80	0.55
48	26	0.148	0.018	137.12	35.48	0.72

Table S3. Linear regression analysis of average force of unconfined cells versus spread areas for each type of stiffness reported in Figure 1 D.

Stiffness ($\text{nN}/\mu\text{m}$)	Slope ($\text{nN}/\mu\text{m}^2$)	Slope Error ($\text{nN}/\mu\text{m}^2$)	Intercept (nN)	Intercept Error (nN)	R^2
11	-0.00034	0.00053	4.21	0.64	0.01
15	-0.00068	0.00035	4.54	0.44	0.11
24	-0.00144	0.00042	9.41	0.74	0.28
31	-0.00056	0.00048	7.78	0.88	0.04
48	-0.00163	0.00093	15.12	1.82	0.12

Table S4. Fit coefficients of spread areas of cells as a power-law function of effective modulus (coefficient \pm standard deviation) shown in Figure 1 E. Coefficients were compared with rat aortic smooth muscle cells (RASMCs) from Engler *et al.* (2004). The values for RASMC were adapted by assuming that the polyacrylamide gel is a homogenous, isotropic linear elastic material with a Poisson's ratio of 0.5, such that $G_{eff} = E/3$, where E is the elastic modulus of the gel measured by atomic force microscopy nano-indentation.

$Area = BG_{eff}^N$		
	N	B
HPAEC – 12h	0.43 ± 0.11	1155 ± 72
RASMC – 4h	0.29	5501
RASMC – 24h	0.37	8258

Table S5. Linear regression analysis of average forces of unconfined cells versus substrate stiffness shown in Figure 1 F.

$Slope (\mu m)$	$Slope Error (\mu m)$	$Intercept (nN)$	$Intercept Error (nN)$	R^2
0.254	0.027	1.89	0.47	0.81

Table S6. Sample size of cells studied in confined cell study in Figure 3 and regression coefficients for total forces vs. area, average forces vs. area, and average forces vs. stiffness used in Figure 3. A total of 258 cells were measured. (* Pearson's r for power fit was done by performing linear fit in log-log scale).

$Area (\mu m^2)$		Stiffness ($nN/\mu m$)				linear regression in Fig. 3A			regression in Fig. 3B $AF = a \times Area^b$		
						$Slope (nN/\mu m^2)$	$Intercept (nN)$	R^2	a	b	R^2
	11	13	16	13	9	0.043	36.32	0.98	27.14	-0.25	0.94
	15	7	14	9	8	0.048	33.61	0.86	22.49	-0.22	0.94
	24	8	14	9	6	0.081	78.40	0.96	51.70	-0.24	0.99
	31	17	23	21	19	0.101	74.26	0.94	59.59	-0.25	0.99
	48	20	13	12	7	0.122	148.5	0.76	241.0	-0.39	0.99
linear regression in Fig. 3C	$Slope (\mu m)$	0.44	0.33	0.25	0.23						
	$Intercept (nN)$	0.47	0.49	1.81	1.46						
	R^2	0.86	0.67	0.88	0.41						

Table S7. Nonlinear regression analysis of average force of unconfined cells versus spread areas using a power-fit of $Average\ force = a \times Area^b$, shown in Figure 1 D. Pearson's r for power fit was calculated by performing linear fit on the data in log-log scale.

Stiffness ($nN/\mu m$)	a	Error in a	b	Error in b	R^2
11	8.27	8.33	-0.11	0.15	0.01
15	10.25	5.85	-0.15	0.09	0.11
24	92.87	36.8	-0.36	0.06	0.48
31	38.36	29.9	-0.24	0.11	0.08
48	99.94	67.8	-0.30	0.1	0.19

Table S8. Sample size of cells studied in confined cell study in 3T3 and regression coefficients for total forces (TF) vs. area, average forces (AF) vs. area, and average forces vs. stiffness used in Figure S2. A total of 173 cells were measured. (* R-squared value for power fit was done by performing linear fit in log-log scale).

Area (μm^2)		441 900 1521 2304				linear regression in TF vs. Area			regression in AF vs. Area $AF = a \times \text{Area}^b$		
						Slope ($\text{nN}/\mu\text{m}^2$)	Intercept (nN)	R^2	a	b	R^2
Stiffness ($\text{nN}/\mu\text{m}$)	15	8	23	13	9	0.021	35.47	0.96	26.99	-0.31	0.94
	24	3	13	15	6	0.015	36.85	0.99	60.44	-0.42	0.99
	32	2	14	22	2	0.035	48.91	0.97	41.73	-0.29	0.99
	48	3	19	20	9	0.059	76.57	0.96	92.07	-0.34	0.99
linear regression in AF vs. Stiffness	Slope (μm)	0.21	0.16	0.15	0.16						
	Intercept (nN)	0.74	1.16	0.37	-0.88						
	R^2	0.87	0.92	0.89	0.94						

Table S9. Sample size of cells studied in confined cell study in HA-SMC and regression coefficients for total forces vs. area, average forces vs. area, and average forces vs. stiffness used in Figure S3. A total of 182 cells were measured. (* Pearson's r for power fit was done by performing linear fit in log-log scale).

Area (μm^2)		441 900 1521 2304				linear regression in TF vs. Area			regression in AF vs. Area $AF = a \times \text{Area}^b$		
						Slope ($\text{nN}/\mu\text{m}^2$)	Intercept (nN)	R^2	a	b	R^2
Stiffness ($\text{nN}/\mu\text{m}$)	15		14	14	13	0.032	32.89	0.91	27.2	-0.28	0.98
	24	2	18	16	9	0.059	25.97	0.98	25.5	-0.22	0.97
	32	5	23	15	9	0.041	75.83	0.99	107.5	-0.41	0.94
	48	2	19	18	5	0.078	74.21	0.97	31.0	-0.18	0.94
linear regression in AF vs. Stiffness	Slope (μm)	0.23	0.13	0.14	0.13						
	Intercept (nN)	2.03	2.24	1.41	1.09						
	R^2	0.98	0.94	0.96	0.97						

Table S10. Regression coefficients for total focal adhesion area vs. cell area and average focal adhesion (FA) area vs. cell area used in Figure 5 A and B.

<i>Stiffness</i> (nN/ μm)	<i>linear regression in Fig. 5 A</i>			<i>regression in Fig. 5 B</i> <i>FA Area = a \times Area^b</i>		
	<i>Slope (1)</i>	<i>Intercept</i> (μm^2)	<i>R</i> ²	<i>A</i>	<i>b</i>	<i>R</i> ²
11	0.017	4.92	0.90	3.57	-0.14	0.76
15	0.016	7.86	0.59	4.69	-0.17	0.40
24	0.017	9.73	0.88	6.56	-0.20	0.96
31	0.017	10.96	0.98	8.27	-0.24	0.98
48	0.015	24.35	0.96	48.98	-0.44	0.99

Table S11. Regression coefficients for average FA area vs. stiffness used in Figure 5 C.

<i>Cell area</i> (μm^2)	<i>linear regression</i>		
	<i>Slope</i> ($\mu\text{m}/\text{nN}$)	<i>Intercept</i> (μm^2)	<i>R</i> ²
441	0.033	1.02	0.52
900	0.030	0.88	0.92
1521	0.016	1.04	0.79
2304	0.006	1.20	0.48

Table S12. Nonlinear regression analysis of average focal adhesion area of confined cells with respect to substrate stiffness and spread area shown in Figure 5 D. The model fit function is *Average FA Area = (a \times Area^b) \times (c + d \times Stiffness)*. Coefficients were calculated numerically with 28 model evaluations and 11 derivative evaluations.

<i>a</i>	<i>B</i>	<i>c</i>	<i>d</i>	<i>R</i> ²
2.59	-0.253	2.14	0.06	0.841

SI Materials and Methods

Traction Force Micropost Arrays. Arrays of microposts were manufactured via replica molding of polydimethylsiloxane (PDMS) using a mixing ratio of 10:1 for the base and curing agent (Sylgard 184, Dow Corning). The deflection of a post (δ) was used to determine the local traction force (F) of a cell according to $F = k\delta = (3\pi Ed^4/64h^3)\delta$ where k is the spring constant of a post, d is its diameter, h is its height, and E is the elastic modulus of PDMS. A scanning electron microscope (FEI Sirion) was used to measure the dimensions of the microposts (Table S1). The elastic modulus of PDMS specimens baked for 3 h at 110 °C were measured to be $E = 2.49 \pm 0.17$ MPa according to ASTM standard D412. The effective shear modulus of a micropost array, which represents the overall compliance of the array, was determined according to $G = (\pi Ed^4/32s^2h^2)$, where s is the spacing between the posts (1).

Microcontact Printing. After stamping, the arrays were immersed in 2 $\mu\text{g/ml}$ Δ^9 -DiI solution (Invitrogen) for 1 h to stain the PDMS so that the posts could be observed with fluorescent microscopy. After staining, the arrays were submerged in 0.2% Pluronic F-127 solution (Sigma-Aldrich) for 1 hr to block adhesions to the side-walls and bottom surface of the arrays.

Immunofluorescent Staining. After culturing cells on the arrays for 14 hours, the samples were submerged in an ice-cold buffer containing 10 mM PIPES (J.T.Baker), 50 mM NaCl (BDH), 150 mM sucrose (J.T.Baker), 2 mM PMSF (Electron Microscopy Sciences) and 3 mM MgCl (BDH), 20 $\mu\text{g/ml}$ aprotinin, 1 $\mu\text{g/ml}$ leupeptin, and 1 $\mu\text{g/ml}$ pepstatin (all from G-Biosciences) at pH 6.8 for 1 min to reduce enzymatic activity and maintain cytoskeletal stability. The samples were then strongly permeabilized in the same ice-cold buffer, but with the addition of 0.5% Triton X-100 for 2 min. The samples were then fixed with 4% paraformaldehyde (EMD Chemicals) in PBS and blocked with 10% goat serum (Gibco). The samples were incubated with Hoechst 33342 (Invitrogen), AlexaFluor 488-conjugated phalloidin (Invitrogen), IgG anti-vinculin (hVin1, Sigma Aldrich), and AlexaFluor 647-conjugated anti-IgG antibodies (Invitrogen). The samples were imaged on an inverted fluorescence microscope (Ti-E, Nikon) using a 60 \times , 1.4 NA, oil immersion objective with 400 ms exposure time for vinculin, 200 ms for actin and DiI-labeled posts, and 7 ms for nuclei.

Image analysis of traction forces, spread area, and focal adhesions. The spread area of an unconfined cell on an array was measured from an outline of its actin image. The area of a cell confined to a square island using the stamp-off technique was determined by the expression $((N - 1)s + d)^2$, where N is the number of posts along one side of a cell ($N = 3-9$ posts), and s and d are as defined previously. A diameter of 3 μm was used in this calculation instead of the diameters listed in Table S1. Not every cell filled the area of a square island, so only those cells that filled more than 90% of the posts within a pattern were selected for analysis. Focal adhesions were detected from the vinculin images of each cell by linear filtering to subtract background fluorescence and image thresholding to segment the adhesions, as previously reported (2). Only vinculin structures larger than 0.05 μm^2 in area were quantified as focal adhesions. Total focal adhesion area for a cell was determined by summing the area of its individual focal adhesions. Average focal adhesion area was quantified by dividing total focal adhesion area by the number of posts underneath a cell. The number of adhesions was assumed to be the same as the number of posts. Deflections in the microposts were analyzed as previously described (2) and used to determine the local traction force. From this measurement, the total force of a cells was calculated, which is the sum of the magnitude of traction forces at all posts underneath a cell and is given by $F_{\text{total}} = \sum_N k\delta_n$, where N is the number of posts underneath a cell, k is the stiffness of the posts in the array, and δ_n is the deflection of the n^{th} post of a cell. Since the calculation of total force depends on the number of posts underneath a cell, its value increases with the spread area of a cell. To compare traction forces for cells with different spread areas, average force was quantified by dividing the total force by the number of posts under a cell ($F_{\text{avg}} = F_{\text{total}}/N$).

SI References

1. Rodriguez, A. G., S. J. Han, M. Regnier, and N. J. Sniadecki. 2011. Substrate stiffness increases twitch power of neonatal cardiomyocytes in correlation with changes in myofibril structure and intracellular calcium. *Biophys J* 101:2455-2464.
2. Sniadecki, N. J., A. Anguelouch, M. T. Yang, C. M. Lamb, Z. Liu, S. B. Kirschner, Y. Liu, D. H. Reich, and C. S. Chen. 2007. Magnetic microposts as an approach to apply forces to living cells. *Proc Natl Acad Sci U S A* 104:14553-14558.